

THE MECHANICAL BEHAVIOR OF LARGE FLAWS IN OPTICAL FIBER AND THEIR ROLE IN RELIABILITY PREDICTIONS

G.S. Glaesemann

Corning Incorporated
Corning, New York

Abstract

The flaws in optical fiber of greatest reliability risk are those below the high strength region. The fatigue behavior of proof stress size flaws is similar to that of flaws in the high strength region. The strength of such flaws after aging in 80°C water is markedly different than that of pristine fiber surfaces. Whereas pristine fiber surfaces degrade in strength with aging, large flaws in fiber actually increase in strength with aging. The risk of mechanical failure for fiber in most applications is governed primarily by the fatigue and aging behavior of relatively large flaws.

Introduction

In a previous study, a nearly 400 km fiber strength distribution was statistically scaled for failure probability predictions for a range of fiber lengths in tension and bending.¹ The predicted distributions for the case of bending are replicated in Figure 1. Not surprisingly, for long lengths in tension or bending, such as those found in typical stranded cable designs, the probability of encountering a flaw near the proof stress level is high. Of particular interest are typical short length applications where it is usually assumed only pristine fiber is stressed. By way of example, consider a typical splice enclosure where approximately one meter of fiber is stored in bending. The strength distribution appropriate for this situation is shown in Figure 1. For a common failure probability requirement of 10^{-4} to 10^{-6} , the flaws of greatest risk can be as low as 70 kpsi in strength and are significantly weaker than the strength of pristine fiber (> 500 kpsi). Therefore, regardless of the application, the fatigue and aging behavior of these flaws must be understood in order for engineers to make accurate reliability predictions. The purpose of this paper is to present data on the aging and fatigue behavior of flaws near the proof stress level.

Background

Aging of optical fiber.

The aging of fiber in harsh environments has received much attention in the last few years. Strength degradation of pristine optical fibers after exposure to hot water has been well documented. For example, Figure 2 shows the results of Matthewson and Kurkjian² where pristine silica-clad fiber was strength tested in 2-point bending after

aging in 100°C water. The strength degradation with aging time was attributed to the dissolution of the silica surface. For a pristine fiber surface, as found on short test lengths, aging results in surface roughening and strength degradation.³ This phenomenon is one of flaw introduction for pristine fiber surfaces.

What about the aging of extrinsic flaws in optical fiber, since they are the ones of greatest reliability risk? Little data exists on the aging of the lower strength region of optical fiber strength distributions due to difficulty in finding such flaws with typical strength testing equipment. However, strength increases with aging time have been reported for bulk silica glass.^{4,5} Strength of both abraded and indented silica glass is plotted in Figure 3 versus aging time in silicic acid and water at 90°C. With the exception of indentation cone cracks strength increases of 25 to 35% were measured. Ito and Tomozawa⁴ attributed the strength increase of abraded silica glass to a change in the crack tip morphology best described by "rounding". Rounding of the crack tip leads to a strength increase because it lowers the stress intensity factor over sharp cracks. Marshall and Lawn⁵ argued that a strength increase during aging is caused by relieving of localized residual stresses generated by the indentation or abrasion event. They illustrated their point by showing that the strength increase for indentation cone cracks, produced by sphere on flat glass, is negligibly small. Cone cracks are produced by purely elastic deformation and do not have an associated residual stress field. In this study we will attempt to provide some understanding of the aging behavior of flaws near typical proof stress levels on silica-clad optical fiber.

Fatigue of optical fiber.

Figure 4 is a plot of the fatigue parameter n versus fracture strength for silica-clad fibers and bulk silica glass. The data and references for Figure 4 are summarized in Table 1. This plot is similar to that found in reference 6 with the exception that the data here is confined just to silica fiber and bulk silica glass. The fatigue parameter n for as-received silica-clad fiber is approximately 20 down to strength levels as low as 100 kpsi. The exceptions are n values greater than 25 where extremely slow dynamic fatigue stressing rates were used. Bulk silica glass clearly has n values greater than high strength fiber. Of particular interest are two studies^{10,14} where abraded fibers with strengths less than 100 kpsi demonstrated n values

approaching bulk silica glass as shown in Figure 4. It appears then that there is a transition to higher n values for fiber strengths below 100 kpsi.

Several researchers have argued that the transition to higher n values with lower strengths is a fundamental transition in flaw geometry from a mere surface impression to a more well defined "Griffith" type flaw.^{16,21,22} The technique used to create model flaws in bulk silica glass and optical fiber is that of indentation, where flaws are introduced onto the glass surface using a diamond microhardness indenter.²¹ Results from this technique are shown in Figure 5 where the strength of indentation flaws on fiber and bulk silica glass is plotted versus indentation size. The transition to a more well-defined crack system at an indentation size between 10 and 30 microns is described as moving from a surface impression (subthreshold) to a flaw with well defined radial cracks emanating from the impression (postthreshold) and is characterized by a significant drop in strength. The localized residual stress that accompanies indentation flaws is believed to play a crucial role in the subcritical growth or fatigue of such flaws by assisting in the growth with the end result that subthreshold flaws have a lower measured n (20) than postthreshold flaws (30).¹⁵ This is shown in Figure 6 where measured n values are plotted versus indentation load from reference 15. Postthreshold flaws without the influence of residual stress have measured n values near 40. Comparing the fatigue values in Figure 4 with the strength values in Figure 5 suggests that the indentation flaws near 100 kpsi are subthreshold in form and that the abrasion flaws on fiber near 50 kpsi behave as postthreshold flaws without residual stress.

It has been stated that the residual stress effect on subthreshold flaws does not account for the n of 20 for flaws in the high strength region since the near perfect as-drawn fiber surface is not believed to contain regions of concentrated residual stress.² Also, it has been postulated that the localized residual stress on proof stress level flaws stimulates radial cracks to unexpectedly transition from subthreshold to postthreshold, i.e., "pop-in", during in-service use; and therefore, the ultimate reliability of fiber is ultimately controlled by crack "pop-in" and not subcritical growth of pre-existing flaws.²³ This report will attempt to provide additional fatigue data and understanding of flaws in this strength region.

Experimental Details

Aging.

To examine aging behavior of extrinsic flaws in optical fibers, 125 μm fibers were first mechanically abraded during the drawing process by intentionally touching the fiber with an uncoated 150 μm fiber just before applying a 250 μm dual acrylate coating. The resulting flaws from this abrasion procedure are believed to be more similar to that of blunt indentation, as with the cone indenter for bulk silica in Figure 3. The draw-abraded fibers were aged in 80°C water buffered to pH 7 for up to 60 days. Strength testing of the aged fiber was performed under uniaxial tension in 45% relative humidity and 23°C using a gauge length of 0.5 meters. A strain rate of 70 %/min. was used to minimize crack growth during strength testing. Prior to strength testing all specimens were preconditioned in the test environment for a minimum of 8 hours.

Also included in this study are the aging results from the Honors Thesis by Estep.²⁴ Estep abraded fibers after drawing by chemically removing a one inch section of polymer coating, dropping 30 grams of silica particles onto the fiber surface from a height of 9 cm, and recoating the fiber using a standard fusion-splice recoating apparatus. This abrasion technique is believed to more closely replicate the abrasion or sharp indentation surface conditions in Figure 3 than that of blunt indentation cone cracks. The aging condition for these fibers was 85°C water. The strength testing procedure consisted of baking the fibers at 60°C and a soft vacuum for 24 hours and subsequent loading to failure in less than 15 seconds. This preconditioning procedure was intended to minimize strength degradation during the tensile test.

Fatigue.

For this part of the study draw-abraded fibers were prepared as discussed above. Also, post-draw abraded specimens were prepared using an abrasion process similar to Estep's²⁴. Fibers from both abraded surface conditions were dynamic fatigue tested at 23°C and 100% RH using rates of 0.4, 0.04, 0.004, and 0.0004%/min. A fiber gauge length of 4 meters was used for the dynamic fatigue tests. Also, specimens for fatigue testing were preconditioned a minimum of 2 hours in 100% RH. Fibers from both surface conditions were also aged in 80°C water and fatigue tested in the same manner. A minimum of 10 specimens per strain rate was used for all fibers. For some of the aged draw-abraded fibers a fifth rate of 0.00004%/min was also used to investigate any curvature in the data, but the resulting strengths did not depart from the best fit line of the 4 faster rates.

Results and discussion

Aging.

Strength distributions from the draw-abraded fibers in this study and the post-draw abraded fibers from reference 24 are shown in Figure 7. It is of particular interest that the strengths produced by these abrasion techniques are greater than that needed to produce post-threshold flaws according to the indentation results in Figure 5. It is postulated that indentation flaws model the large flaws in optical fibers. It follows that the flaws with strengths shown in Figure 7 are believed to be subthreshold in morphology.

The tensile strength of the aged abraded fibers is plotted versus aging time in Figure 8. The strength of both abraded fiber types is shown to initially decrease slightly followed by a significant increase in strength to values significantly greater than their initial value. For example, the draw-abraded fiber has an initial strength of 66 kpsi and after 150 days of aging the strength increases to 106 kpsi. The post-draw abraded fiber of Estep starts at 75 kpsi and increases to 133 kpsi after 10 days, a value nearly twice its original strength.

It is interesting that the post-draw abraded fiber increased in strength more rapidly than the draw-abraded. The post-draw abraded reaches 100 kpsi in 10 days, whereas, the draw-abraded attains 100 kpsi after 150 days. One explanation for this difference is that the higher aging temperature for the post-draw abraded fiber, 85°C versus 80°C, simply causes the aging process to proceed at a faster rate. This is unlikely since the published activation energies of 45 to 75 kJ/mol, postulated for the aging process at these temperatures,² greatly underestimate the

observed difference in rate. Another possible explanation is that the aging behavior is dependent on the type of flaw produced by the abrasion method. For example, recall the results in Figure 3 where cone flaw produced by blunt indentation responded more slowly to the aging environment than abrasion and Vickers indentation. It was speculated earlier that draw-abrasion is more reflective of blunt indentation like that produced by a sphere on a flat plate, whereas, post-draw particle abrasion is more similar to sharp indentation. Clearly more research is needed to better understand the aging differences in Figure 8, nevertheless, the strength of abraded fiber increased with aging time irrespective of the flaw introduction method and aging temperature.

Fracture mechanics developed for modelling localized residual stresses around indentations predicts that the maximum strength increase by residual stress relief is twice its original value.²⁵ Measured strength increases for abraded soda-lime glass, known for its ability to retain localized residual stresses, are on the order of only 40% when annealed at 400°C for 3 hours.²⁶ Now in the case of silica, it is well known that the level of residual stress retained in this anomalous glass as a result of surface damage is much less than that of soda-lime glass due to densification of the silica structure during abrasion.^{25,27,28} Silica falls far short of retaining the residual stress needed to produce a doubling in strength after aging. Assuming that fracture mechanics applies to the damage created in this study, the two-fold increase in strength of the post-draw abraded fiber is best explained by a modification of the crack tip geometry by a process like rounding. It is speculated that the smaller strength increase of the draw-abraded fiber is an indication that the flaws are more of a surface impression, a geometry less affected by aging.

The fact that abraded fiber strength increases with aging time suggests that if the abrasion flaws are in fact subthreshold in form, they do not transition from subthreshold into postthreshold form. The transition from subthreshold flaw to postthreshold is characterized by the emanation of radial cracks from the impression region created during abrasion or indentation. Figure 5 shows a strength decrease of nearly one order of magnitude over this transition. The abraded fibers do not experience this transition to lower strengths, rather the strength increases with aging time. Also, considering the fact that the aging environment in this study is more severe than that experienced by fiber in most applications, it is believed that proof stress level flaws in optical fiber are not at risk of catastrophic failure from radial crack "pop-in". Furthermore, the above results also suggest that fracture mechanics modeling of the "pop-in" event may not be necessary for normal fiber proof stress levels.

The increase in abraded fiber strength with aging time is in sharp contrast to that of pristine fiber in Figure 2 which degrades in strength over the same aging period. Evidence of surface roughening has been recently obtained for aged pristine fiber surfaces³ and dissolution of silica has been the most common explanation for the formation of pits on the pristine fiber surface.² This phenomenon of silica dissolution at high temperatures is the same argument proposed by Ito and Tomozawa⁴ for the strengthening of large flaws. Whereas, silica dissolution degrades the strength of pristine fiber through flaw formation, it rounds the tip of preexisting flaws leading to a strength increase. Clearly, the concern over the aging behavior of high strength fiber cannot be extended to flaws near the proof stress.

It also is worth noting that the variability in strength appears to increase with aging time and higher strengths for both abraded fibers. Estep²⁴ suggests that this increase in variability with increasing strength is a further indication crack tip rounding. He argues that one would expect the overall magnitude of the flaw depth distribution to decrease with rounding, but a relative difference between flaws in specimens to remain.

Fatigue.

The strength distributions of draw and post-draw abraded fibers used for fatigue testing are shown in Figure 9. Abrading on the draw provides a relatively uniform strength distribution just above a typical proof stress level of 50 kpsi with a Weibull modulus, m , of 13. Post-draw particle abrasion yields a distribution of strength values just below 50 kpsi and modulus of 9. Figure 10 is a dynamic fatigue plot for the post-draw abraded fibers. The best fit line through all the data is shown and the calculated n value of 20.4 was obtained. A similar analysis of the draw-abraded fiber yielded an n value of 23.4. The results from dynamic fatigue testing draw-abraded and post-draw abraded fibers are plotted in Figure 11 along with large flaw fatigue data from Table I. Also included in Figure 11 is fatigue data for fiber abraded to 20 kpsi. The error bars on n were determined from the 95% confidence interval of the slope of the best fit line through the dynamic fatigue data. The results from this study do not agree with data from other studies on fiber abraded to 50 kpsi where n values equal to that of bulk silica glass were measured. Rather, results from this study match the fatigue of subthreshold flaws and abraded fibers with strengths of 100 kpsi.

The reason for the difference between the results for flaws near 50 kpsi from this study and the previously published results at 50 kpsi is not clear. However, if one were to hold to the fracture mechanics framework developed for indentation type flaws, the 50 kpsi flaws with high n values would be postthreshold in form and, as previously discussed, the flaws in this study are subthreshold, even though the strengths are the same. If postthreshold flaws in fiber are possible, then one would expect that a further abrasion of the fiber in this study would eventually provide such a flaw. The achievement would be marked by a decrease in strength and a dramatic increase in n over the present results near 20. To test this argument, fibers were abraded to 20 kpsi using the post-draw particle abrasion method and the fatigue testing yielded an n of 32. This data point is shown as a triangle in Figure 11. This increase in n from 23 to 32 is the same as shown in Figure 6 for the transition from subthreshold to postthreshold flaws.

The dynamic fatigue behavior of the 50 kpsi draw-abraded fiber is plotted in Figure 12 versus aging time in 80°C water. The n value increases from an initial 23 to 40 after 20 days of aging, but with further aging decreases to approximately 27. Due to the significant uncertainty in n it is difficult to determine if an actual increase in n has been realized. Interestingly, an increase in n from 23 to 27 is approximately what one would predict from residual stress relief that comes with aging of subthreshold flaws.^{29,30}

The data presented on n of aged abraded fiber is important because it enables those making reliability predictions to have a certainty about n over 30 year life on the flaws that matter most; namely, those near the proof stress level. There are two reasons for this statement. First, in the

previous section on strength after aging of abraded fiber it was concluded that one need not be concerned about strength degradation due to phenomena other than fatigue. Secondly, the fatigue data presented here shows that an n value in the low 20s is conservative even after exposure to a severe aging environment.

Summary

- Flaws produced by particle abrasion or draw abrasion are a convenient means for examining the mechanical behavior of proof stress level flaws.
- Large flaws in silica-clad optical fiber do not exhibit the zero-stress-aging strength degradation found on pristine fiber surfaces. Results confirm a process of strengthening with aging attributed to a modification of the flaw tip geometry.
- The fatigue behavior of large flaws is at least maintained with aging.
- The mechanical reliability of optical fiber is best served by continued study of the large flaw region. This is consistent with failure probability requirements, the experimental findings in this and other studies, and the most likely application of fiber (cabling, installation, termination, and long-term life of long fiber lengths)

Acknowledgments

The author would like to thank M.G. Estep for his helpful discussions, D.J. Walter and D.A. Clark for their experimental work and patience, R.L. Bennett and T.L. Jacoby for developing the draw-abrasion technique, and to D.R. Powers and R.V. VanDewoestine for their support and guidance.

References

1. G.S. Glaesemann, "Optical Fiber Failure Probability Predictions from Long-Length Strength Distributions," pp.819-825 in proceedings of the 40th International Wire and Cable Symposium, St. Louis, Mo., 1991.
2. M.J. Matthewson and C.R. Kurkjian, "Environmental Effects on the Static Fatigue of Silica Optical Fiber," *J. Am. Ceram. Soc.*, **71** [3] 177-83 (1988).
3. R.S. Robinson and H.H. Yuce, "Scanning Tunneling Microscopy of Optical Fiber Corrosion: Surface Roughness Contribution to Zero-Stress Aging," *J. Am. Ceram. Soc.*, **74** [4] 814 (1991).
4. S. Ito and M. Tomozawa, "Crack Blunting of High-Silica Glass," *J. Am. Ceram. Soc.*, **65** [8] 368-371 (1982).
5. D.B. Marshall and B.R. Lawn, "Surface Flaws in Glass," in: *Strength of Inorganic Glass*, ed. C.R. Kurkjian (Plenum, New York, 1985).
6. C.R. Kurkjian, J.T. Krause, and M.J. Matthewson, "Strength and Fatigue of Silica Optical Fibers," *J. Lightwave Tech.*, **7** [9] 1360-1370 (1989).
7. D. Kalish and B.K. Taryyal, "Static and Dynamic Fatigue of a Polymer-Coated Fused Silica Optical Fiber," *J. Am. Ceram. Soc.*, **61** [11-12] 518-23 (1978).
8. S.P. Craig, W.J. Duncan, P.W. France, and J.E. Sodgrass, "The Strength and Fatigue of Large Flaws in Silica Optical Fibres," in *Proc. 8th ECOC (Cannes, France)*, 1982.
9. G.S. Glaesemann, Masters Thesis, University of Massachusetts, 1983.
10. H.H. Yuce, P.L. Key, and D.R. Biswas, "Investigation of the Mechanical Behavior of Low Strength Fibers," in *Fiber Optics Reliability: Benign and Adverse Environments III*, *Proc. SPIE 1174*, 272-278 (1989).
11. G.S. Glaesemann and S.T. Gulati, "Dynamic Fatigue Data for Fatigue Resistant Fiber in Tension vs. Bending," in 1989 Technical Digest Series, Vol. 5, *Proc Optical Fiber Communication Conference*, 48 (1989).
12. J.E. Ritter, Jr, J.M. Sullivan, and K. Jakus, "Application of Fracture Mechanics Theory to Fatigue Failure of Optical Glass Fibers," *J. Appl. Phys.*, **49** [9] 4779-82 (1978).
13. F.A. Donaghy and D.R. Nicol, "Evaluation of the Fatigue Constant n in Optical Fibers with Surface Particle Damage," *J. Am. Ceram. Soc.*, **66** [8] 601-4 (1983).
14. S. Sakaguchi and Y. Hibino, "Fatigue in Low-Strength Silica Optical Fibers," *J. Mater. Sci.*, **19**, 3416-20 (1984).
15. T.P. Dabbs and B.R. Lawn, "Strength and Fatigue Properties of Optical Glass Fibers Containing Microindentation Flaws," *J. Am. Ceram. Soc.*, **68** [11] 563-69 (1985).
16. M.J. Matthewson, "Strength and Reliability of Fused Silica Optical Fiber," *BROADBAND (FOC/LAN) '90* (Baltimore, MD.), 1990.
17. J.E. Ritter, Jr., and C.L. Sherburne, "Dynamic and Static Fatigue of Silicate Glasses," *J. Am. Ceram. Soc.*, **54** [12] 601-605 (1971).
18. S.T. Gulati, "Mechanical Properties of SiO₂ versus SiO₂-TiO₂ Bulk Glasses and Fibers," in proceedings of 1991 MRS Fall Meeting, Boston.
19. S.M. Wiederhorn, A.G. Evans, and D.E. Roberts, pp. 829-41 in *Fracture Mechanics of Ceramics, Vol. 2*. Edited by R.C. Bradt, D.P.H. Hasselman, and F.F. Lange. Plenum Press, New York, 1974.
20. S. Sakaguchi, Y. Sawaki, Y. Abe, and T. Kawasaki, "Delayed Failure in Silica Glass," *J. Mat. Sci.*, **17**, 2878-86 (1982).
21. T.P. Dabbs, D.B. Marshall, and B.R. Lawn, "Flaw Generation by Indentation in Glass Fibers," *J. Am. Ceram. Soc.*, **63** [3-4] 224-25 (1980).
22. K. Jakus, J.E. Ritter, Jr, S.R. Choi, T.J. Lardner, and B.R. Lawn, "Failure of Fused Silica Fibers with Subthreshold Flaws," *J. Non-Cryst. Sol.*, **102** 82-87 (1988).
23. F.A. Donaghy and T.P. Dabbs, "Subthreshold Flaws and Their Failure Prediction in Long-Distance Optical Fiber Cables," *J. Lightwave Tech.*, **6** [2] 226-32 (1988).

24. M.G. Estep, "The Effects of Zero Stress Aging on the Strength of Large Flaws Introduced to the Surface of Optical Waveguides," Honors Thesis, New York State College of Ceramics at Alfred University, Alfred, New York, 1990.
25. M.A. Israel, J.E. Ritter, Jr., and K. Jakus, "Strength and Dynamic Fatigue Behavior and Indented Borosilicate and Soda-Lime Glasses," *Phy. and Chem. Glass.*, **28** [4] 133-38 (1987).
26. D.H. Roach and A.R. Cooper, "Effect of Contact Residual Stress Relaxation on Fracture Strength of Indented Soda-Lime Glass," *J. Am. Ceram. Soc.*, **68** [11] 632-36 (1985).
27. C.R. Kurkjian, "Mechanical Stability of Oxide Glasses," *J. Non-Cryst. Sol.*, **102**, 71-81 (1988).
28. J.T. Hagan, "Cone Cracks around Vickers Indentations in Fused Silica Glass," *J. Mat. Sci.* **14**, 462-66 (1979).
29. S.R. Choi, J.E. Ritter, Jr., and K. Jakus, "Failure of Glass with Subthreshold flaws," *J. Am. Ceram. Soc.*, **73** [2] 268-74 (1990).
30. D.B. Marshall and B.R. Lawn, "Flaw Characteristics in Dynamic Fatigue: The Influence of Residual Contact Stresses," *J. Am. Ceram. Soc.*, **63** [9-10] 532-536 (1980).

Table I. Summary of Fatigue Data for Silica-Clad fiber and Bulk Silica Glass.

Silica form	Surface Condition	Strength (kpsi)	n		RH (%) *	comments	ref.	
			crack velocity	dynamic fatigue				static fatigue
fiber	as-drawn	700		15.9	14.3	97	tension	7
fiber	as-drawn	800		25.5		amb.	tension	8
fiber	as-drawn	800		22.5		water	tension	8
fiber	as-drawn	700		22		water	tension	9
fiber	as-drawn	700		21.1	19.7	45	tension	10
fiber	as-drawn	700		22.1		water	bending	11
fiber	as-drawn	530		29.9		water	bending	11
fiber	as-drawn	600		20.8		100	tension	11
fiber	as-drawn	420		25.5		100	tension	11
fiber	as-drawn	700		21.7		amb.	tension	12
fiber	abraded	180		22.1	19.8	50	tension	13
fiber	abraded	150		22.3	20.2	45	tension	10
fiber	abraded	80		26	22.2	45	tension	10
fiber	abraded	50		33.7		45	tension	10
fiber	abraded	50			35.6	water	tension	14
fiber	abraded	50		42.6		60	tension	14
fiber	abraded	100		20.5		water	tension	8
fiber	abraded	100		25.5		amb.	tension	8
fiber	indented	70		19		water	tension	15
fiber	indented	100		20		amb.	sub-threshold	16
bulk	indented	10		30.7		water	sub-threshold	15
bulk	abraded	14		37.8		water		17
bulk	abraded	10		45		water		18
bulk	compact tension		42			water		14
bulk	DCB		36			100		19
bulk	compact tension		36-44			20 to 24 to 70 °C		20

* test temperatures 20 - 25 °C except where otherwise noted.

Figure 1. Failure Probability Predictions for Optical Fiber in Bending.

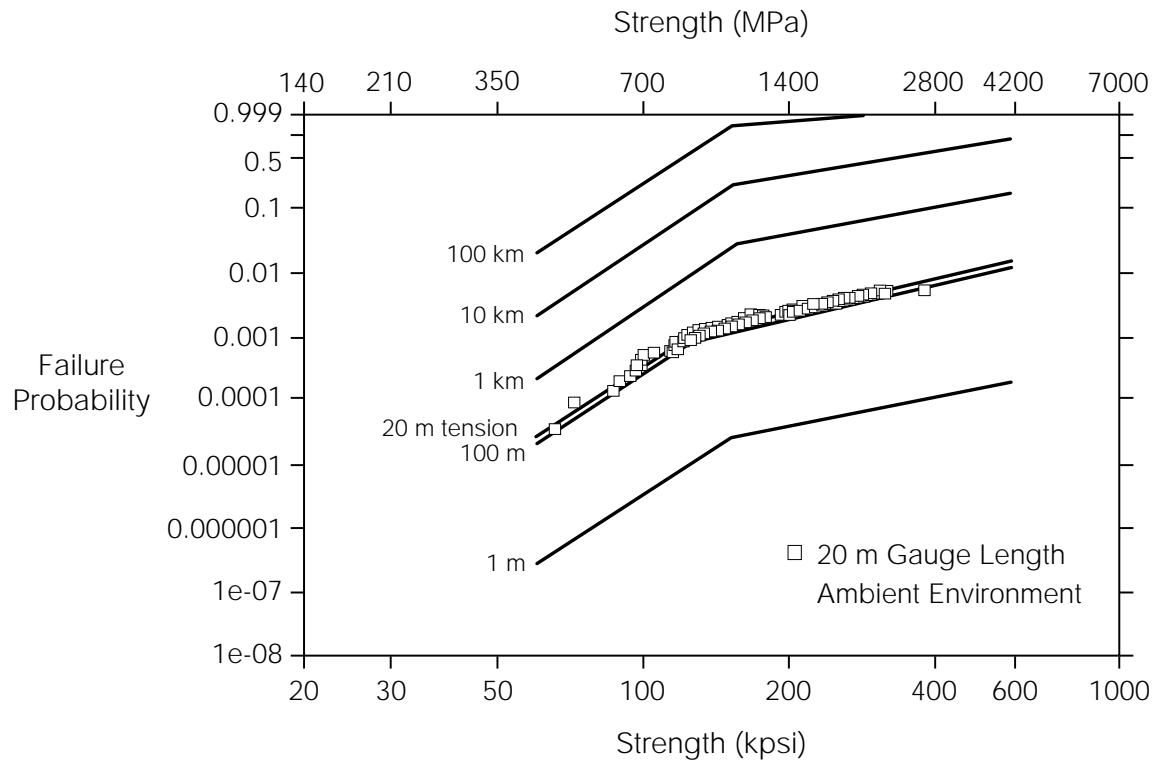


Figure 2. Effect of Aging on the Strength of Optical Fiber. From Ref. 2.

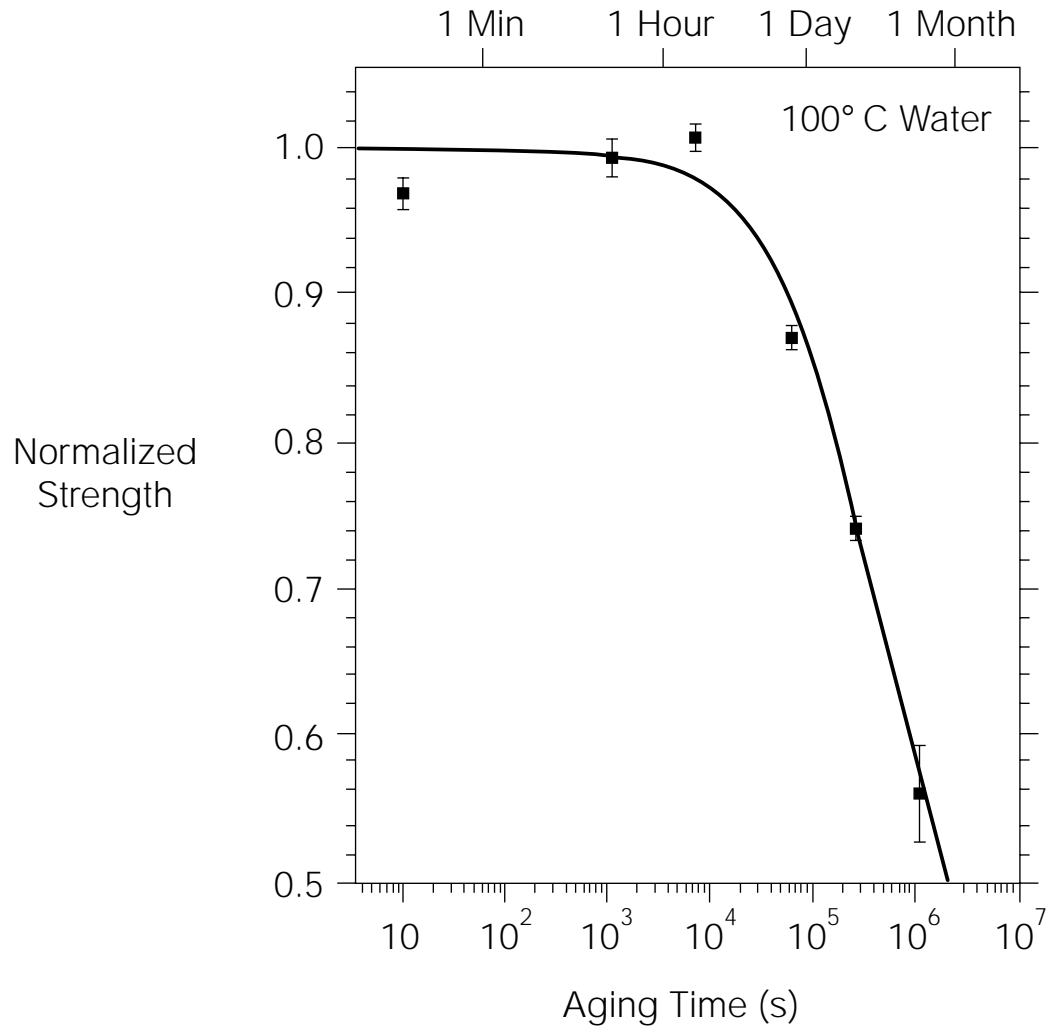


Figure 3. Fracture Strength of High Silica Glass as a Function of Aging Time in 90 °C Silicic Acid. From Ref. 5.

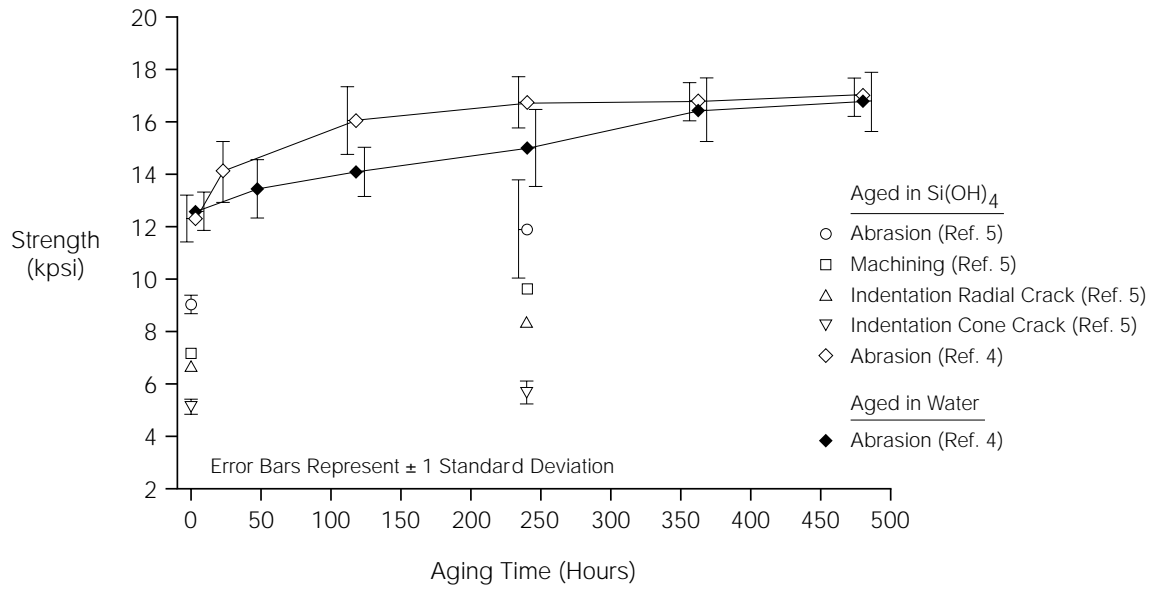


Figure 4. Fatigue Susceptibility n of Silica. References and Data in Table I.

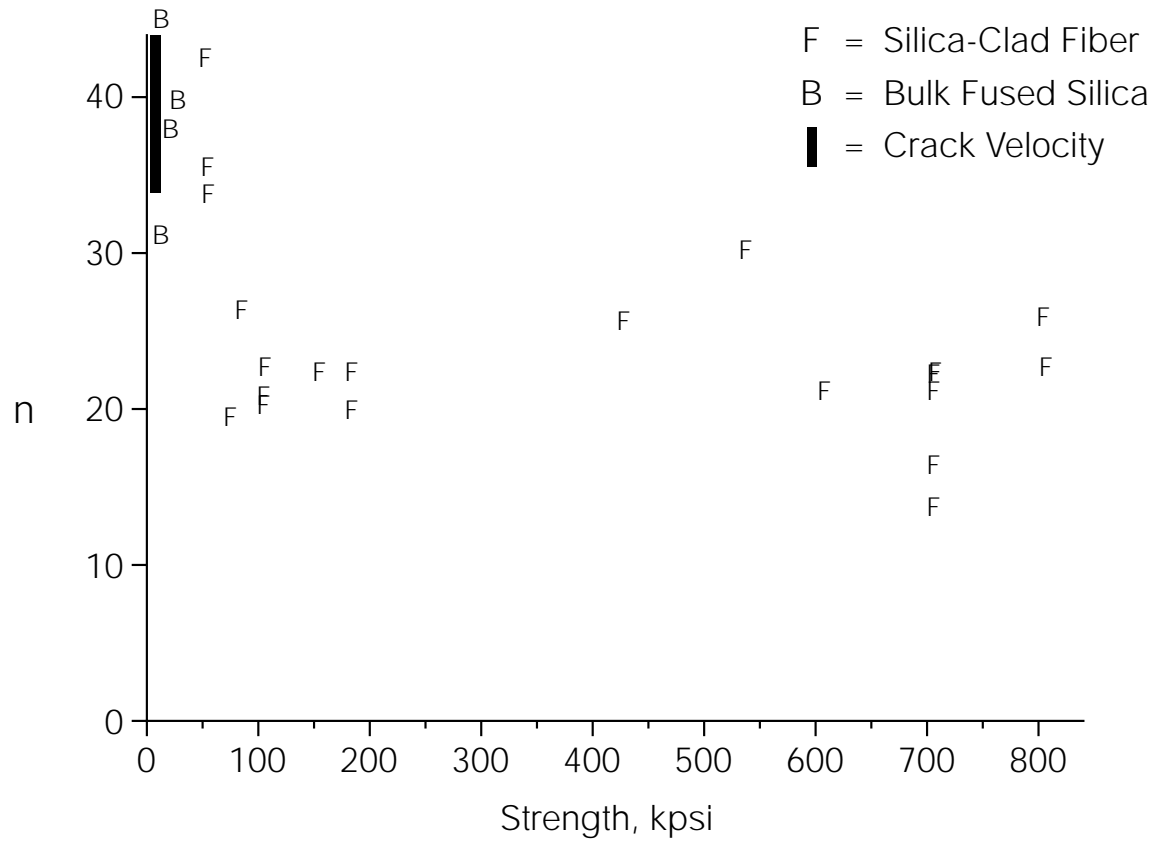


Figure 5. Strength of Indented Silica-Clad fibers and Bulk Silica Glass.

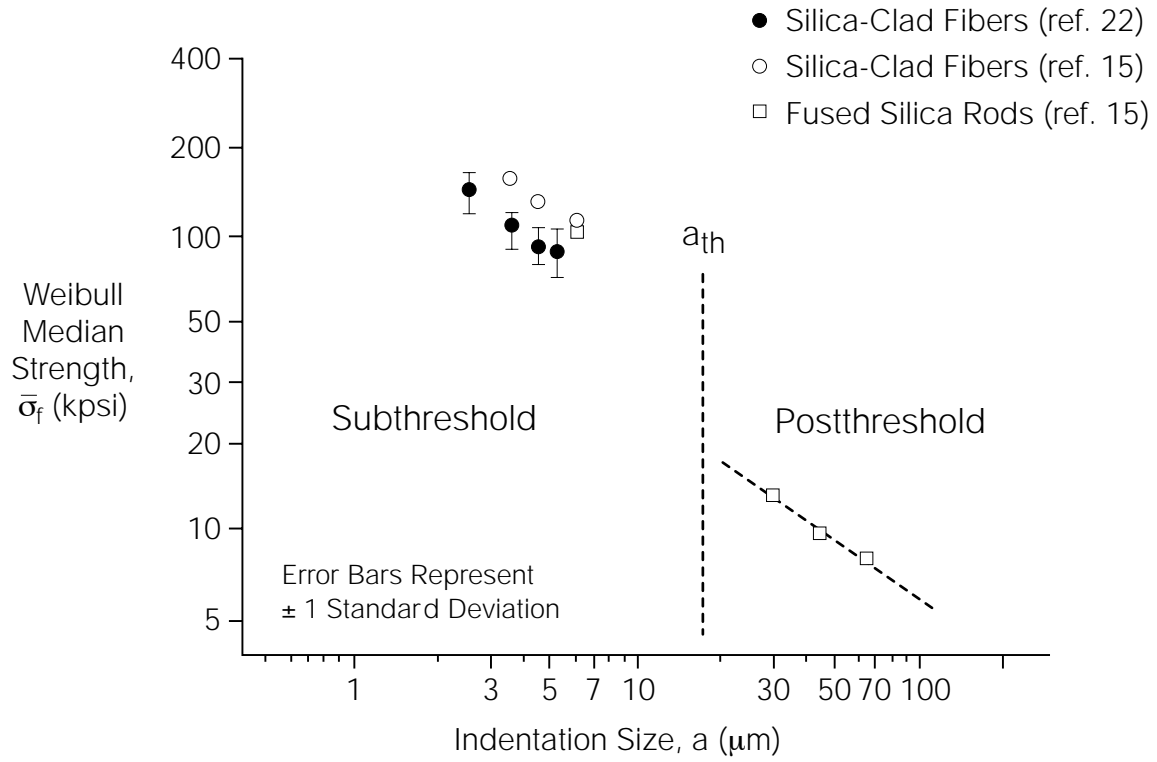


Figure 6. Plot of n for Indentation Flaws in Silica.

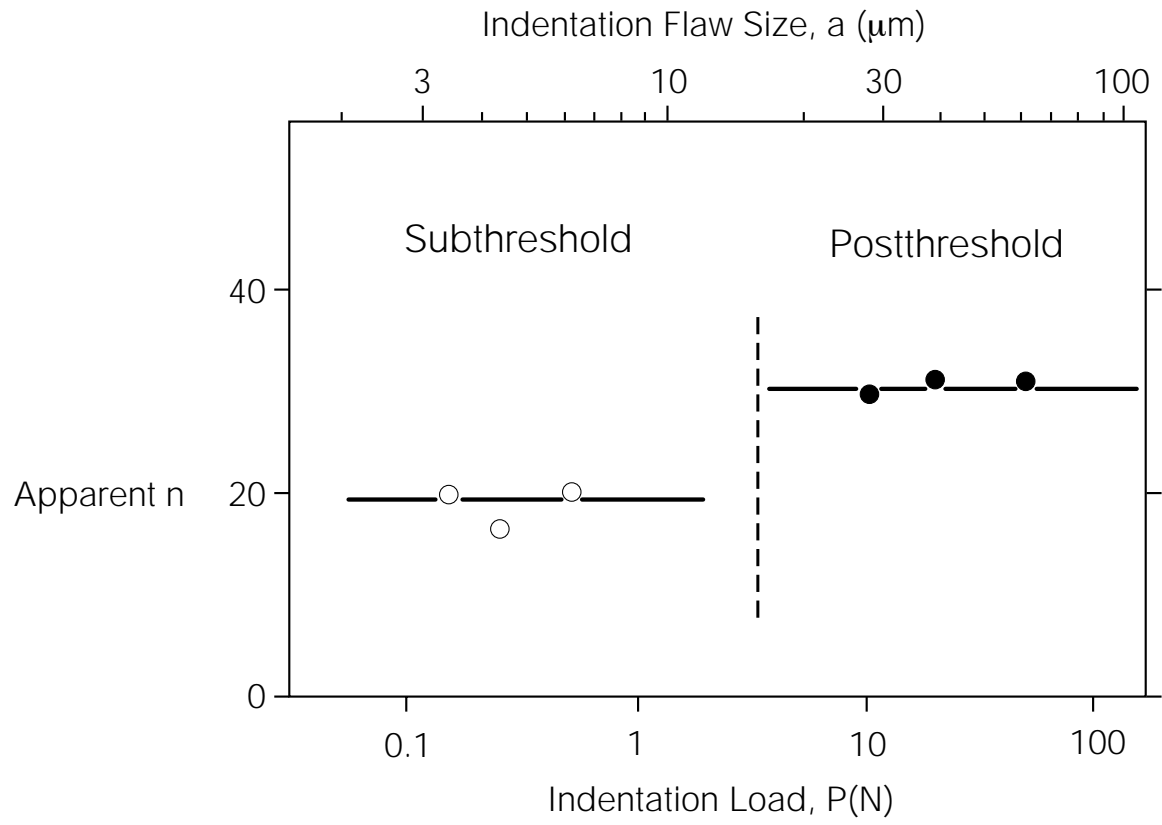


Figure 7. Strength of Abraded Silica-Clad Fibers.

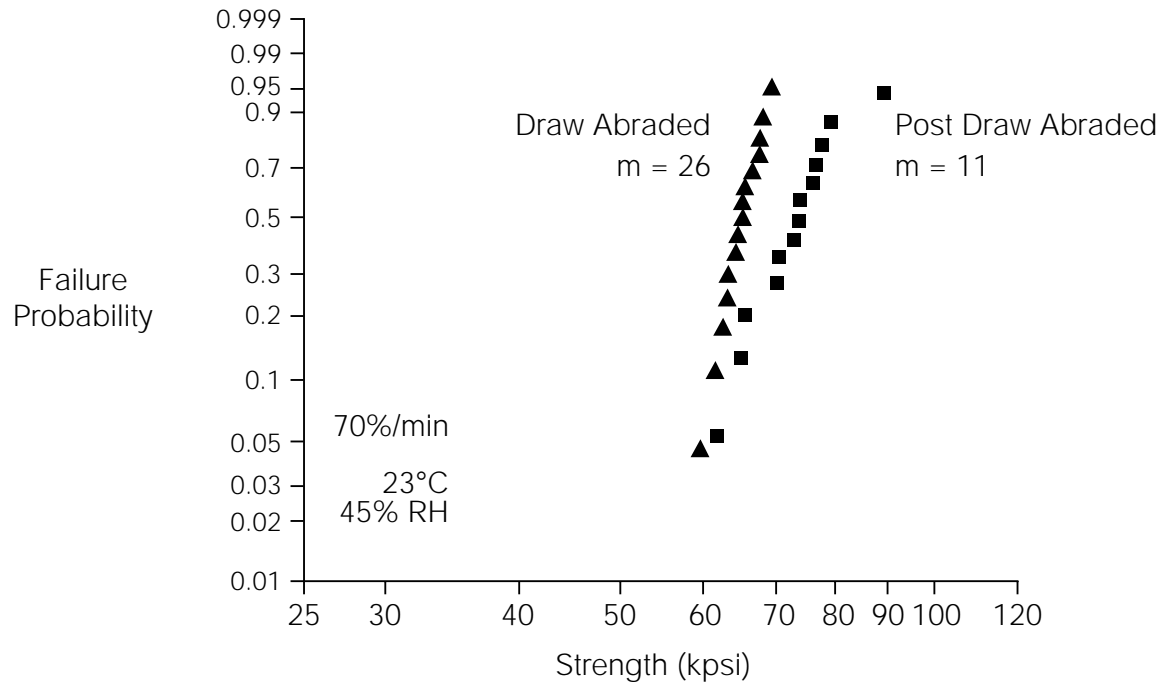


Figure 8. Strength of Abraded Silica-Clad Fiber as a Function of Aging Time in 80 °C Water.

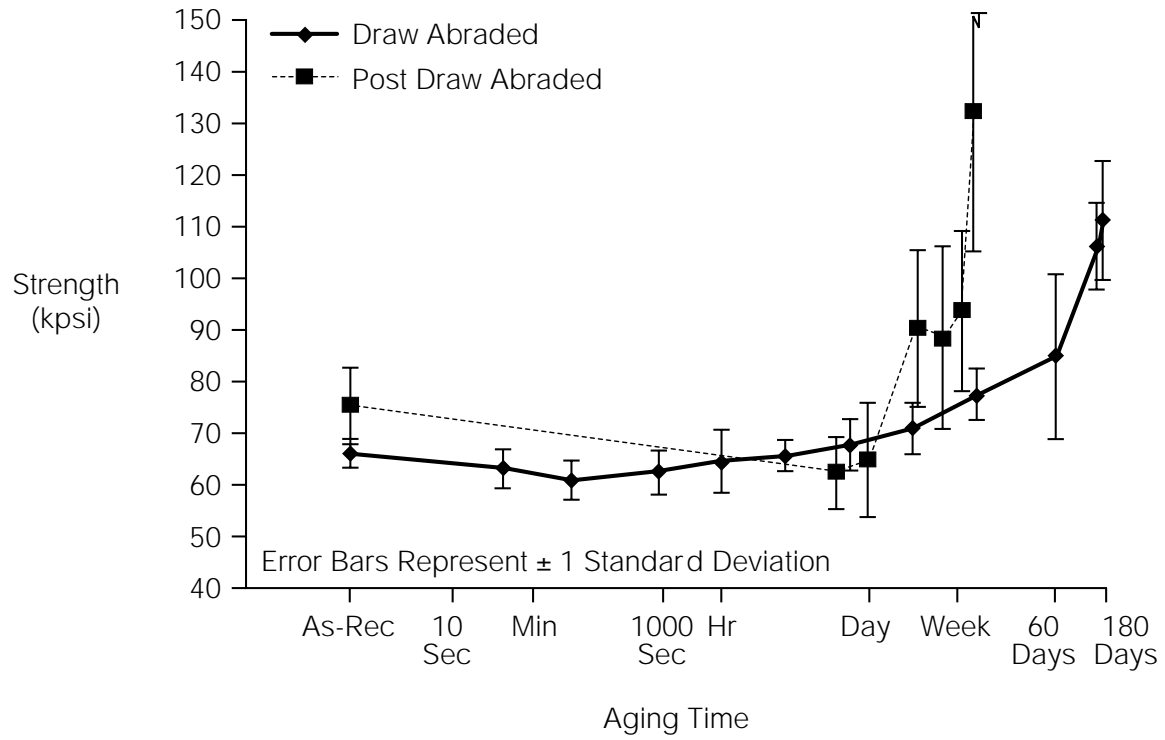


Figure 9. Strength of Abraded Silica-Clad Fibers for Fatigue Testing.

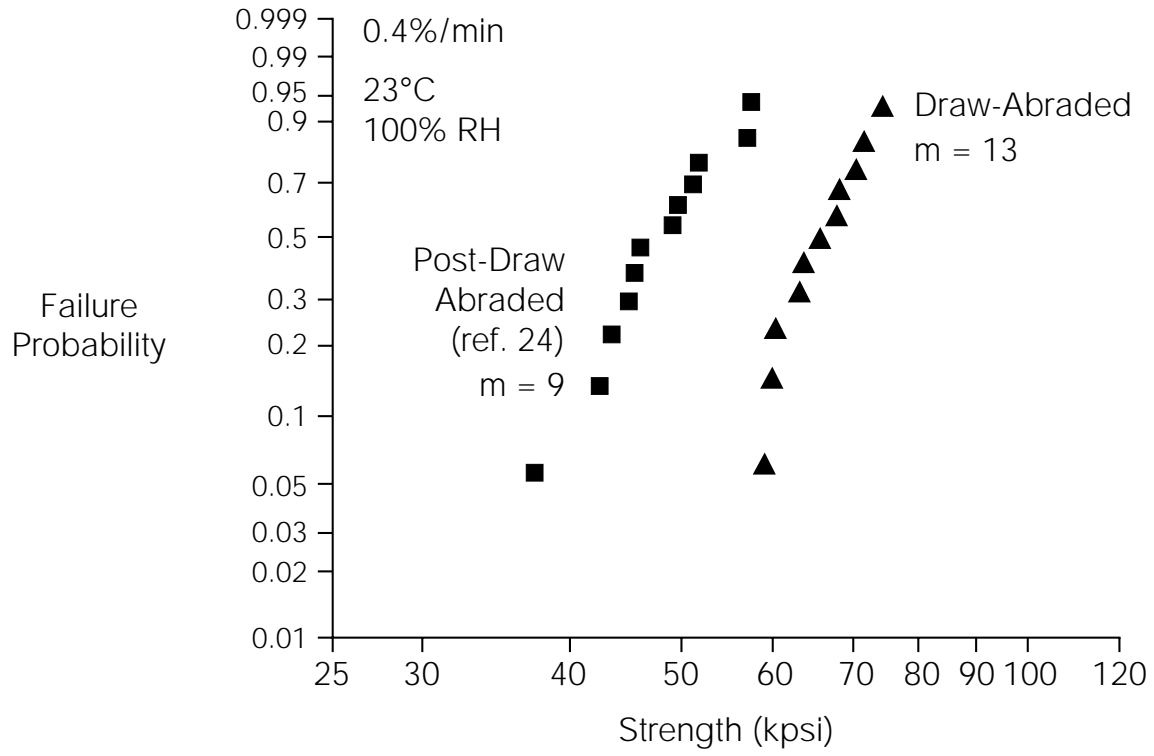


Figure 10. Dynamic Fatigue of Post-Draw Abraded Silica-Clad Fiber.

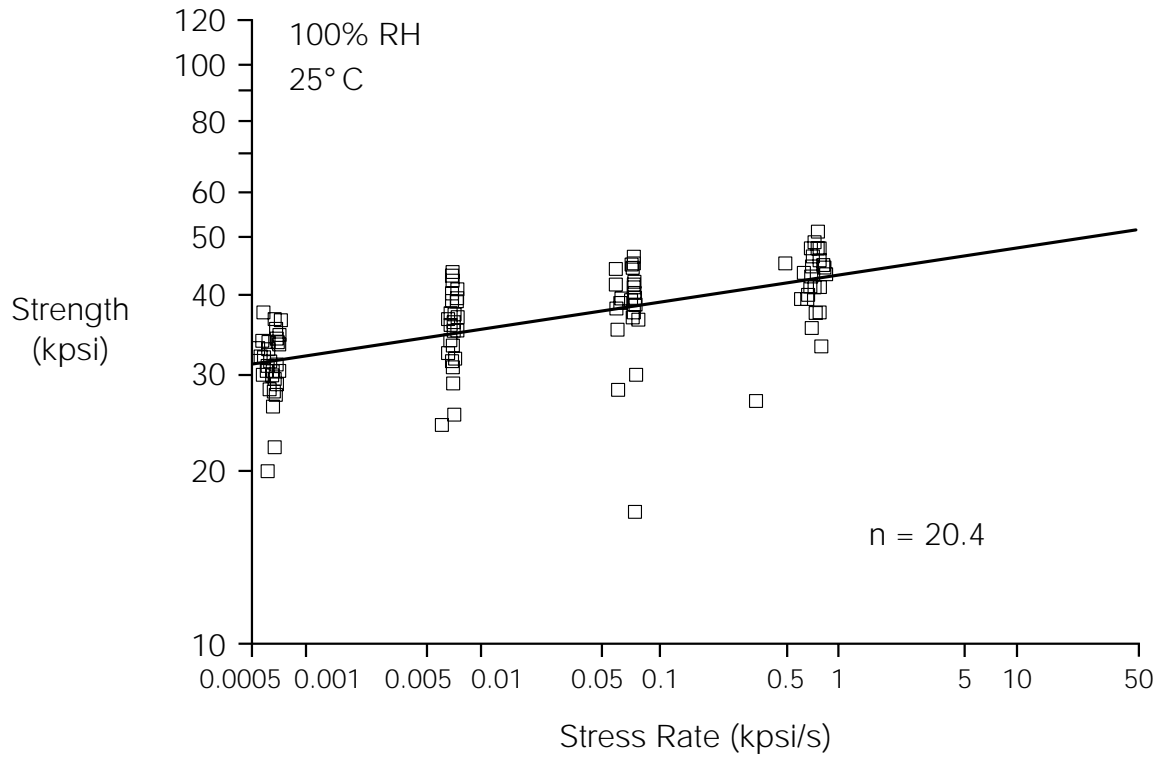


Figure 11. Fatigue Susceptibility n of Abraded Silica-Clad Fibers.

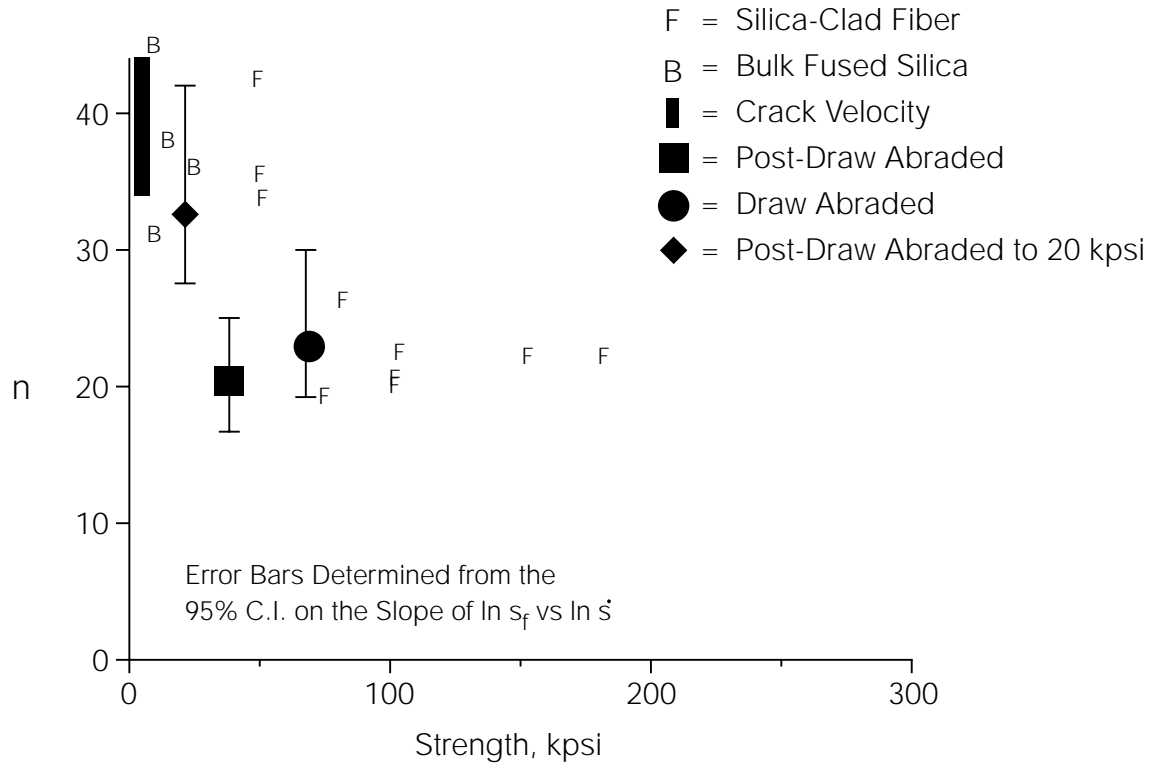
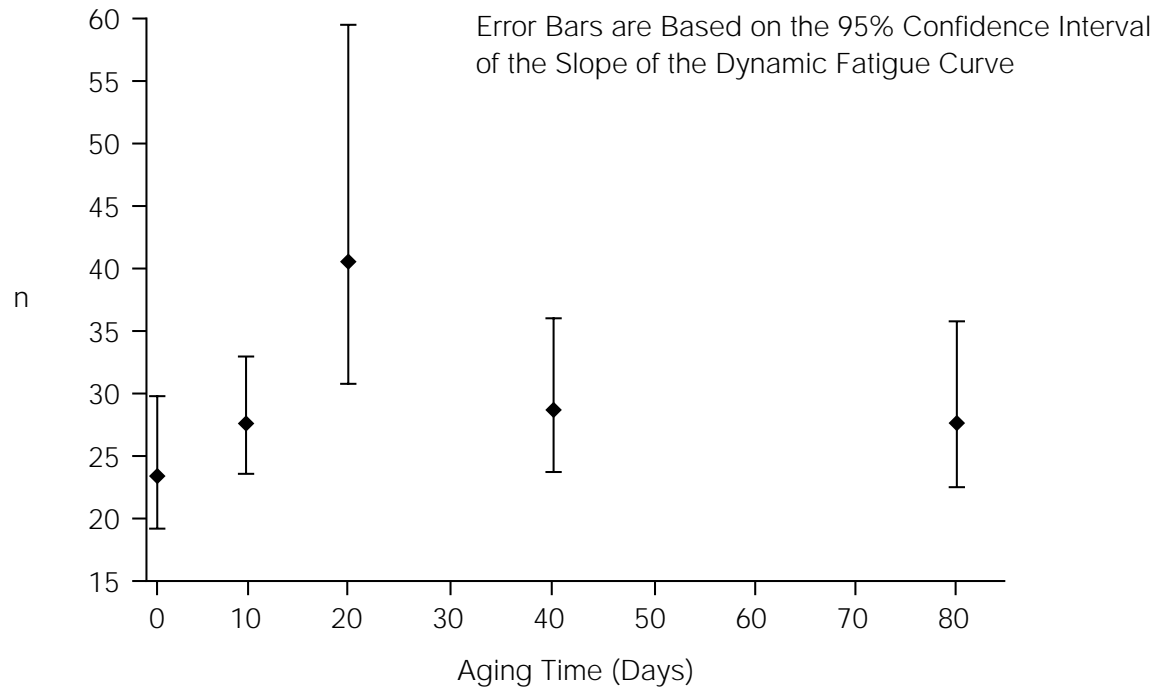


Figure 12. Effect of Aging in 80°C Water on n of Draw-Abraded Silica-Clad Fibers.



G. Scott Glaesemann, SP-DV-01-8 Corning Inc., Corning, N.Y., 14831. Glaesemann is a senior development engineer responsible for the optical fiber strength laboratory at Corning. His research focuses on the mechanical properties and reliability of optical fiber. He has been employed by Corning for six years at the Sullivan Park technology facility. Glaesemann received his master's degree and Ph.D. in mechanical engineering from the University of Massachusetts and a B.S. in mechanical engineering from North Dakota State University.